Jagunal is required for reorganizing the endoplasmic reticulum during *Drosophila* oogenesis

Sangil Lee[1] and Lynn Cooley[1,2,3]

[1]Department of Genetics and [2]Department of Cell Biology, Yale University School of Medicine, New Haven, CT 06520
[3]Department of Molecular Cellular and Developmental Biology, Yale University, New Haven, CT 06511

Vesicular traffic in the *Drosophila melanogaster* oocyte occurs actively during vitellogenesis. Although endocytosis in the oocyte has been well characterized, exocytic vesicular traffic is less well understood. We show that the oocyte endoplasmic reticulum (ER) becomes concentrated into subcortical clusters during vitellogenesis. This ER reorganization requires Jagunal, which is an evolutionarily conserved ER membrane protein. Loss of Jagunal reduces vesicular traffic to the oocyte lateral membrane, but does not affect posterior polarized vesicular traffic, suggesting a role for Jagunal in facilitating vesicular traffic in the subcortex. Reduced membrane traffic caused by loss of Jagunal affects oocyte and bristle growth. We propose that ER reorganization is an important mechanism used by cells to prepare for an increased demand for membrane traffic, and Jagunal facilitates this process through ER clustering.

Introduction

The ER is a three-dimensional membranous network that extends throughout the cell, and is organized into discrete domains: the nuclear envelope, the smooth ER, and the rough ER. The ER participates in a variety of cellular functions, such as protein and lipid synthesis, the regulation of intracellular calcium levels, degradation of glycogen, and detoxification reactions (Baumann and Walz, 2001). The fine structure of the ER in any given cell may be organized depending on which of these functions predominates. For example, during myogenesis, the ER differentiates into the sarcoplasmic reticulum, which is an ER specialized in Ca^{2+} regulation (Flucher, 1992). Proteins and lipids synthesized in the ER are transported to their destinations by the secretory pathway, and different cells use the secretory pathway to varying degrees. In addition, the amount of exocytic vesicular traffic may vary in a cell during development.

Drosophila melanogaster oogenesis is a good model system to study how cells prepare for the varying requirements of vesicular transport activity. The *D. melanogaster* oocyte is interconnected with 15 nurse cells by ring canals (Fig. 1 A; Robinson and Cooley, 1996), and cytoplasm transported from nurse cells to the oocyte constitutes a major contribution to oocyte growth (Mahajan-Miklos and Cooley, 1994). Another source for oocyte growth is yolk taken up during vitellogenesis (stages 8–10), when the oocyte becomes highly endocytic. During vitellogenesis, the rate of oocyte growth overtakes the rate of nurse cell growth such that, ultimately, the oocyte volume equals the total volume of the 15 nurse cells. In addition, a high density of microvilli forms on the oocyte surface during these stages (Mahowald, 1972). Therefore, a large amount of membrane must be added to the oocyte plasma membrane during vitellogenesis. However, mechanisms for increasing exocytic membrane trafficking is poorly understood.

In this study, we identified a novel gene, *jagunal*, which is required for oocyte and bristle growth. The *jagunal* gene encodes a novel conserved ER membrane protein. We show that Jagunal is required for reorganizing the ER through ER clustering in the oocyte during vitellogenesis. The failure to reorganize the ER in *jagn* mutant oocytes results in reduced vesicular traffic and slowed cell growth. We propose that Jagunal is involved in reorganizing the ER in cells that must increase exocytic membrane traffic during development.

Results

Germline clones of *jagunal* exhibit defects in oocyte integrity and growth during stages 10 and 11

After the completion of vitellogenesis, the *D. melanogaster* oocyte doubles its volume within 30 min to reach its maximum size (Fig. 1 A). The final growth of the oocyte depends on rapid cytoplasm transport from nurse cells. Mutations that affect the ability of nurse cells to transport cytoplasm result in the

Correspondence to Lynn Cooley: Lynn.cooley@yale.edu

Abbreviations used in this paper: GLC, germline clone; PDI, protein disulfide isomerase.

The online version of this article contains supplemental material.

The Journal of Cell Biology, Vol. 176, No. 7, March 26, 2007 941–952
http://www.jcb.org/cgi/doi/10.1083/jcb.200701048

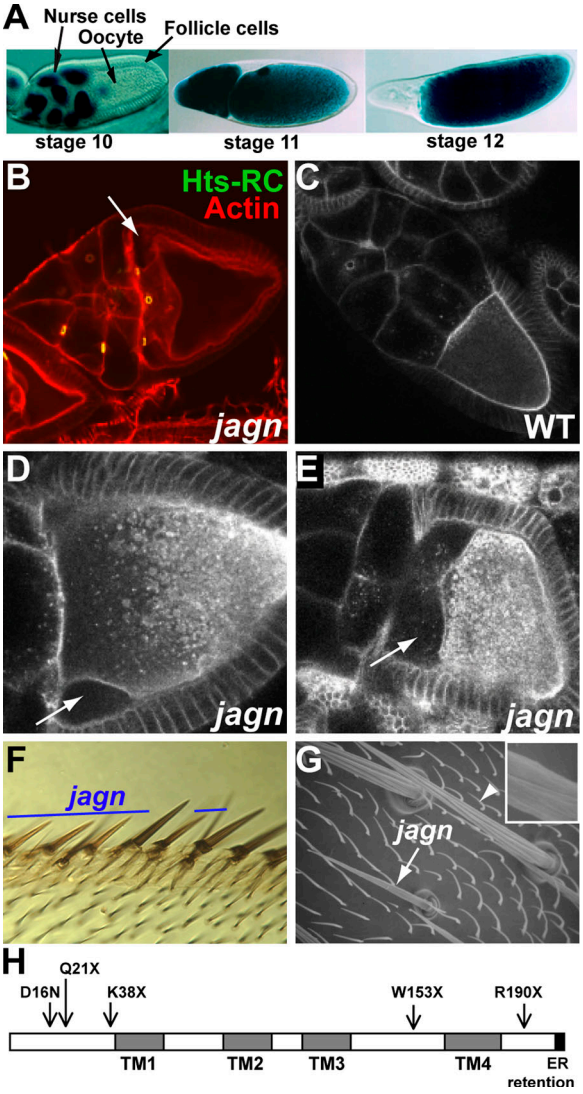

Figure 1. **Jagunal is required for oocyte and bristle growth.** (A) *D. melanogaster* egg chambers. Egg chambers before (stage 10), during (stage 11), and after (stage 12) nurse-cell dumping are shown with nuclear lacZ staining. Egg chambers are composed of germline cells (15 nurse cells and the oocyte) surrounded by somatic follicle cells. All egg chamber images are oriented with anterior to the left. (B) $jagn^{Q21X}$ GLCs were stained with rhodamine-conjugated phalloidin (red) to visualize F-actin and Hts-RC antibodies (green) to visualize ring canals. Mutant oocytes detach from nurse cells and follicle cells at the anterior region (arrow). (C–E) Live egg chambers were examined by Bsg-GFP fluorescence, which reveals plasma membranes and vesicles throughout the ooplasm. Wild-type egg chambers (C) and $jagn^{Q21X}$ GLCs (D and E) are shown. Mutant oocytes detach from nurse cells and follicle cells at the anterior region (D, arrow), and the defect becomes more severe as oogenesis proceeds (E, arrow). (F) $jagn^{Q21X}$ clones were marked by *yellow* (y^-). Mutant wing anterior margin bristles are thinner and shorter than their wild-type counterparts. (G) A scanning electron microscope image of wild-type (arrowhead) and $jagn^{Q21X}$ (arrow) microchaetes. Mutant microchaetes are thinner and shorter than wild-type microchaetes, and have weak ridges (inset in G). (H) Domains of Jagunal and mutation sites in *jagn* alleles. Jagunal contains four predicted transmembrane domains (TMs) and a putative ER retention motif (dilysine motif) at the C-terminal end. Mutation sites in all *jagn* alleles were identified in the open reading frame of the *jagunal* gene (CG10978). $jagn^{Q21X}$ is the original mutation isolated from the Lehmann collection, and the other four alleles were isolated from a noncomplementation lethal screen.

production of small eggs (Mahajan-Miklos and Cooley, 1994); this phenotype has been referred to as "dumpless." To identify essential genes involved in oocyte growth, we examined a collection of lethal mutations on chromosome 3R that were made (Yohn et al., 2003) and preselected for a small egg phenotype in Ruth Lehmann's laboratory at New York University (New York, NY). We found a mutation that severely affects oocyte growth and named it *jagunal* (*jagn*), which means small egg in Korean. Germline clones (GLCs) of *jagunal* ($jagn^{Q21X}$) showed a fully penetrant dumpless phenotype with severe defects in oocyte integrity. Four additional *jagn* alleles were isolated from a noncomplementation screen, three of which were lethal and one ($jagn^{D16N}$) that was semilethal (Fig. 1 H). Homozygous mutant $jagn^{Q21X}$, $jagn^{K38X}$, and $jagn^{W153X}$ animals died during the first and second instar larval stages. GLCs of $jagn^{K38X}$ and $jagn^{W153X}$ showed a dumpless phenotype.

jagn mutant oocytes appeared normal until stage 9. During stage 10, the anterior region of the oocyte began to detach from nurse cells and follicle cells (Fig. 1 B, arrow). We examined the phenotype in live egg chambers using a protein trap line (G413) that produces a GFP fusion with Basigin (Bsg) and labels plasma membranes (Fig. 1 C; Morin et al., 2001). In time-lapse images, Bsg-GFP allowed us to view both rapid oocyte growth caused by intercellular cytoplasm transport from nurse cells, and ooplasm streaming in the oocyte during stage 11 (Video 1, available at http://www.jcb.org/cgi/content/full/jcb.2007001048/DC1). As observed in fixed egg chambers, live *jagn* mutant oocytes expressing Bsg-GFP detached from other cells at the anterior region (Fig. 1 D, arrow). In severely affected mutant egg chambers, the oocyte detached from nurse cells completely and the cytoplasm of nurse cells leaked into the space between nurse cells and the oocyte (Fig. 1 E, arrow; and Video 2). In more mildly affected egg chambers, the oocyte was connected to nurse cells, and intercellular cytoplasm transport proceeded to some extent during stage 11 (Video 3). However, the oocyte failed to grow to its maximum size. GLC phenotypes of *jagunal* were less severe in younger flies, likely because of the perdurance of wild-type gene products expressed before the formation of *jagn* mutant clones. Therefore, we focused on the phenotypes in egg chambers from females at least 7 d old.

Jagunal is required for bristle growth and ridge structure

To determine whether the growth defect caused by *jagn* mutations is oocyte specific, we examined the growth of *jagn* mutant bristles by making somatic cell clones. *jagn* mutant bristles were thinner and shorter than wild-type bristles. This defect was observed in several bristle types: wing anterior margin bristles (Fig. 1 F), microchaetes (Fig. 1 G), and macrochaetes (not depicted). *jagn* mutant bristles also exhibited a defect in their surface structure. During the development of bristles, the plasma membrane forms bulges between the 8–12 actin bundles associated with the plasma membrane, and the secretion of cuticle produces a ridged structure (Overton, 1967). Wild-type bristles contain several parallel ridges with deep valleys between them, whereas *jagn* mutant bristles have a weak ridge structure with shallow valleys (Fig. 1 G, inset).

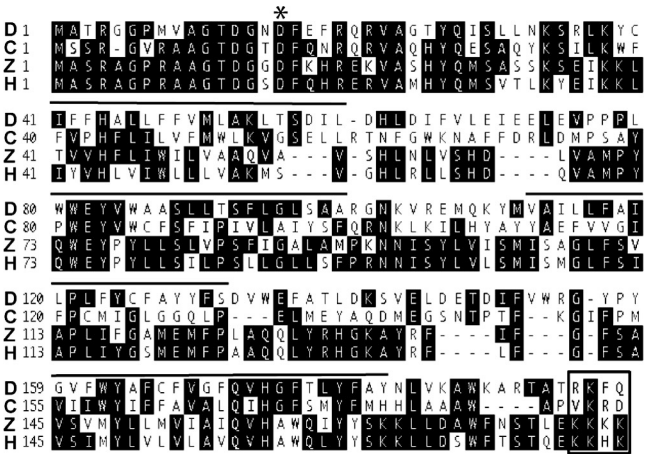

Figure 2. **Alignment of Jagunal homologues.** Jagunal homologues from *D. melanogaster* (NP_649585; D), *C. elegans* (NP_493559; C), zebrafish (NP_001005774; Z), and human (AAH32101; H) are shown. Four predicted transmembrane domains in *D. melanogaster* Jagunal are indicated by lines drawn over the sequence, and a putative dilysine motif at the C-terminal end is indicated by a boxed area. The mutation site in a semilethal allele, *jagn*^{D16N}, is indicated by an asterisk.

The *jagunal* gene encodes a conserved protein with four predicted transmembrane domains

The *jagn* mutation mapped to the chromosome interval 83C1-83D4 as delineated by the proximal breakpoint of the non-complementing deficiency *Df(3)Tp110* and the proximal breakpoint of the complementing deficiency *Df(3R)Tp13*. We mapped the *jagn* mutation further by single-nucleotide polymorphism mapping to within a 70-kb region containing 20 genes. By sequencing open reading frames of genes in the 70-kb interval, we identified mutation sites in all *jagn* alleles within a predicted gene, *CG10978* (Fig. 1 H). The viability and fertility defects associated with all *jagn* alleles were rescued by ubiquitous expression of a *CG10978* cDNA, confirming that *CG10978* is *jagn*.

CG10978 (*jagn*) encodes a protein of 197 amino acids with predicted homologues in the genomes of human, mouse, zebrafish, mosquito, and *Caenorhabditis elegans* (Fig. 2). *D. melanogaster* Jagunal shows 31% identity and 51% similarity to the human homologue. The first 40 amino acids of Jagunal are highly conserved, and a semilethal allele, *jagn*^{D16N}, is a missense mutation at a conserved Asp residue in the N-terminal region (Fig. 2, asterisk), suggesting that the N-terminal region has an important function. The protein has four predicted transmembrane domains and a putative dilysine motif at the C-terminal end (Fig. 2, boxed area). The dilysine motif is known to be an ER-retention motif for ER membrane proteins (Jackson et al., 1993). Jagunal homologues in human and zebrafish match the consensus of the motif (KKXX), whereas arginine replaces lysine in *D. melanogaster* Jagunal (RKXX). However, the C-terminal sequence is likely to act as an ER retention motif; some substitutions of lysine by arginine are permitted in the dilysine motif (Teasdale and Jackson, 1996), and interference with this sequence in Jagunal alters its localization (see the following section).

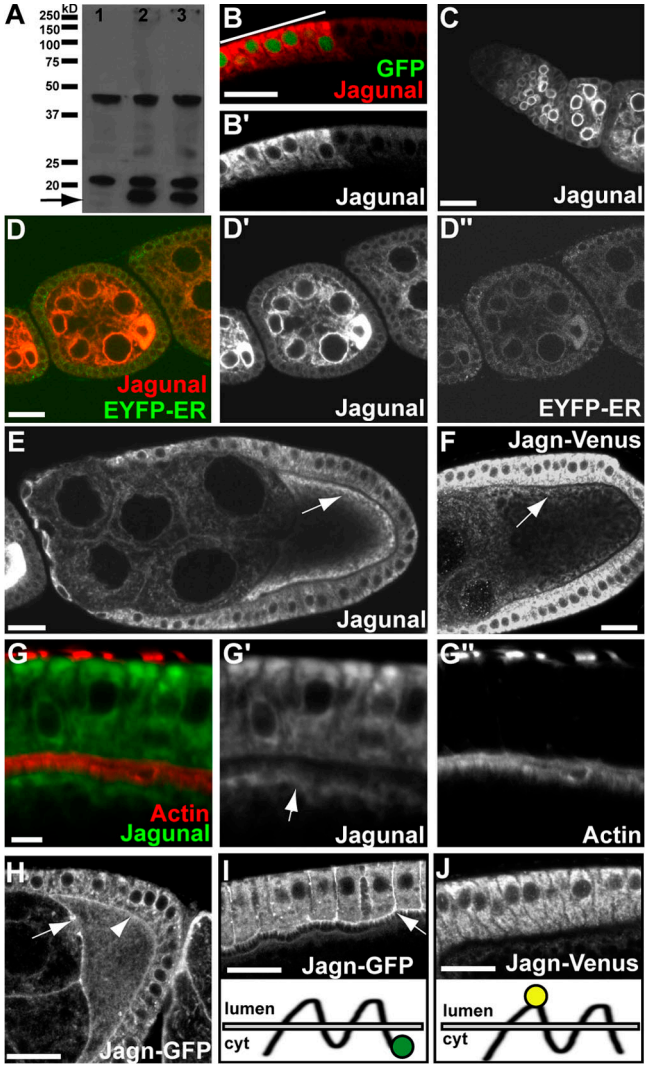

Figure 3. **Localization of Jagunal in egg chambers.** (A) Western blot analysis of wild-type (lane 1) and Jagunal-overexpressing (lanes 2 and 3) ovary extracts. The actin-Gal4 driver (lane 2) and germline triple drivers (lane 3) were used to overexpress Jagunal in the ovary. In wild-type extract, two nonspecific bands were detected, but endogenous Jagunal was barely visible. However, overexpressed Jagunal was detected (arrow). (B and B′) Jagunal-overexpressing follicle cells were marked with GFP (indicated by a bar). Jagunal expression was elevated in GFP-positive cells (red). The follicle cells are shown with the basal membrane at the top. (C–E and G) Jagunal was overexpressed using the actin-Gal4 driver. (C) Jagunal is enriched at the nuclear envelope during early stages. (D–D″) Egg chambers expressing EYFP-ER (green) were stained for Jagunal (red). Jagunal colocalizes with EYFP-ER and becomes enriched in the oocyte during early stages. (E and G) Jagunal becomes enriched at the oocyte subcortex during stages 9 and 10 (arrows). (G–G″) Jagunal enriched at the oocyte subcortex (arrow) is near cortical actin, but does not colocalize with cortical actin. (F and J) Localization of Jagn-Venus in egg chambers. For the Jagn-Venus construct, Venus was inserted between the first and second transmembrane domains (J, bottom). Jagn-Venus localizes at the ER. (H and I) Localization of Jagn-GFP in egg chambers. For the Jagn-GFP construct, GFP was fused to the C terminus (I, bottom). In addition to ER localization, Jagn-GFP localizes at the plasma membrane of follicle cells (I, arrow) and the oocyte (H, arrowhead), including ring canals (H, arrow). Localization of Jagn-GFP to follicle cell plasma membrane is specific to stage 10. Bars: (A–F and H–J) 20 μm; (G) 5 μm.

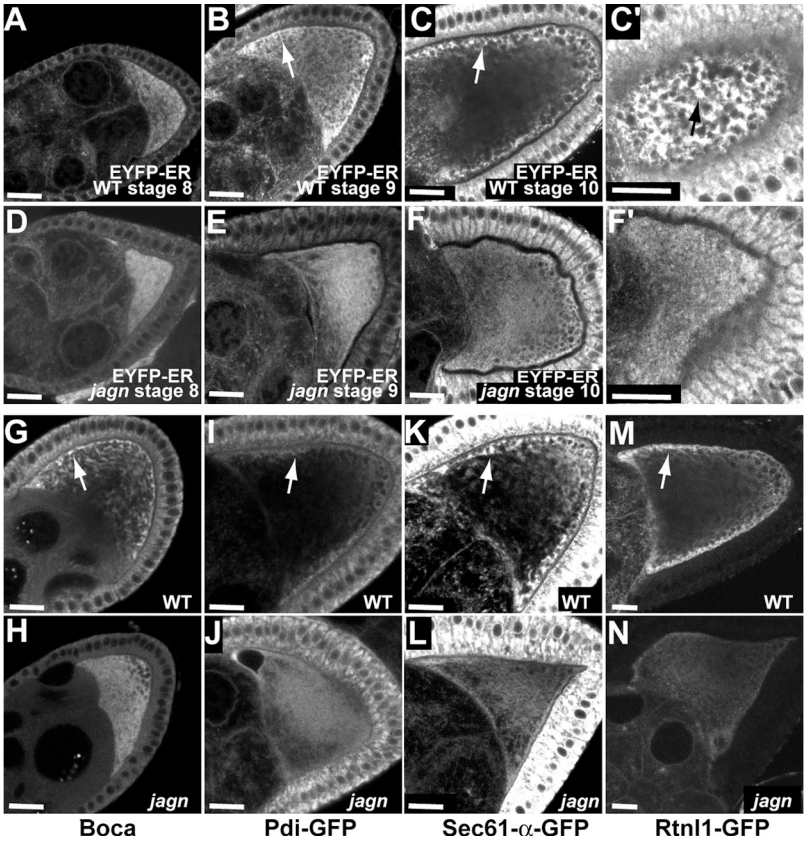

Figure 4. **Jagunal is required for the enrichment of ER proteins in the oocyte subcortical region during vitellogenesis.** (A–F) The distribution of EYFP-ER in progressive stages of wild-type egg chambers (A–C) and *jagn*^{Q21X} GLCs (D–F). Until stage 8, EYFP-ER distributes uniformly in wild-type oocytes (A). However, EYFP-ER becomes enriched in the oocyte subcortex during stages 9 and 10 (B and C, arrows). (C′) A focal plane near the cortex of the oocyte shown in C shows that EYFP-ER is concentrated into clusters in the oocyte subcortex (arrow). (D–F) Until stage 8, EYFP-ER distributes normally in *jagn* mutant oocytes (D). However, EYFP-ER remains dispersed in *jagn* mutant oocytes, with very little subcortical enrichment during stages 9 and 10 (E and F). (F′) A focal plane near the cortex of the oocyte shown in F shows that EYFP-ER distributes uniformly without forming clusters in the oocyte subcortex. (G–N) The distribution of ER proteins Boca (G and H), PDI-GFP (I and J), Sec61-α-GFP (K and L), and Rtnl1-GFP (M and N) in wild-type egg chambers and *jagn*^{Q21X} GLCs. Similar to EYFP-ER, these ER proteins become enriched in the subcortical region in wild-type oocytes (G, I, K, and M, arrows). The enrichment of these proteins in the subcortex is reduced in *jagn* mutant oocytes (H, J, L, and N). Bars, 20 μm.

Jagunal is an ER membrane protein and enriched in the oocyte subcortex during vitellogenesis

To examine the subcellular localization of Jagunal, we made an antibody against Jagunal. Unfortunately, the antibody did not detect endogenous Jagunal proteins in ovaries by Western blotting or immunofluorescence. However, overexpressed Jagunal was detected (Fig. 3, A and B), and because ectopic expression of Jagunal rescued the lethality of *jagn* mutations, the localization of ectopically expressed Jagunal likely reflects that of endogenous Jagunal. In Western blot analysis, overexpressed Jagunal migrated slightly faster than the expected molecular weight of 23 kD on a denaturing gel (Fig. 3 A, arrow); several background bands were also detected. In immunofluorescence, a strong signal was detected in cells overexpressing Jagunal (Fig. 3 B). Jagunal colocalized with an ER marker, EYFP-ER (EYFP fused to the KDEL ER retention sequence; Fig. 3 D; LaJeunesse et al., 2004). Moreover, the distribution of Jagunal showed a characteristic ER pattern during early stages, where it was enriched at the nuclear envelope (Fig. 3, C and D). Jagunal began to be enriched in the oocyte during stages 2–3, where it was uniformly distributed in the cytoplasm (Fig. 3 D). During stages 9 and 10, Jagunal became concentrated in the oocyte subcortex adjacent to follicle cells (Fig. 3, E and G). Double labeling revealed that Jagunal was on the cytoplasmic side of cortical actin filaments in the oocyte (Fig. 3 G, arrow).

Jagn-GFP and -Venus fusion proteins provided evidence for a functional ER retention motif. We made Jagn-GFP and -Venus transgenes by using a genomic DNA construct with GFP fused in-frame to the C-terminal end of Jagunal and with Venus fused in-frame between the first and second transmembrane domains, respectively (Fig. 3, I and J). Because the expression level of these proteins in ovaries was low, we used a GFP antibody to detect them. Jagn-Venus showed an ER distribution and was enriched in the oocyte subcortex (Fig. 3 F), whereas Jagn-GFP localized at the plasma membrane, including ring canals and the oocyte plasma membrane (Fig. 3 H, arrow and arrowhead), in addition to the apparent ER localization. The aberrant localization of Jagn-GFP at the plasma membrane was also found in follicle cells during stage 10, when vesicular traffic occurs actively (Fig. 3 I). In contrast, Jagn-Venus did not localize at the plasma membrane of follicle cells (Fig. 3 J). The aberrant localization of Jagn-GFP at the plasma membrane likely results from loss of ER retention activity because GFP blocks the dilysine motif that must occupy the extreme C-terminal position to be functional (Nilsson et al., 1989). In addition, the Jagn-Venus transgene, but not the Jagn-GFP transgene, rescued the lethality of *jagn* alleles, further supporting the role of the dilysine motif in controlling the localization of Jagunal.

Jagunal is required for establishing subcortical ER in the oocyte during vitellogenesis

The fact that Jagunal is an ER membrane protein suggested that defects caused by *jagn* mutations might be caused by a defect in the ER. Therefore, we examined the distribution of several ER proteins in wild-type and *jagn* mutant oocytes. In wild-type egg chambers, EYFP-ER, which is an ER luminal protein, was

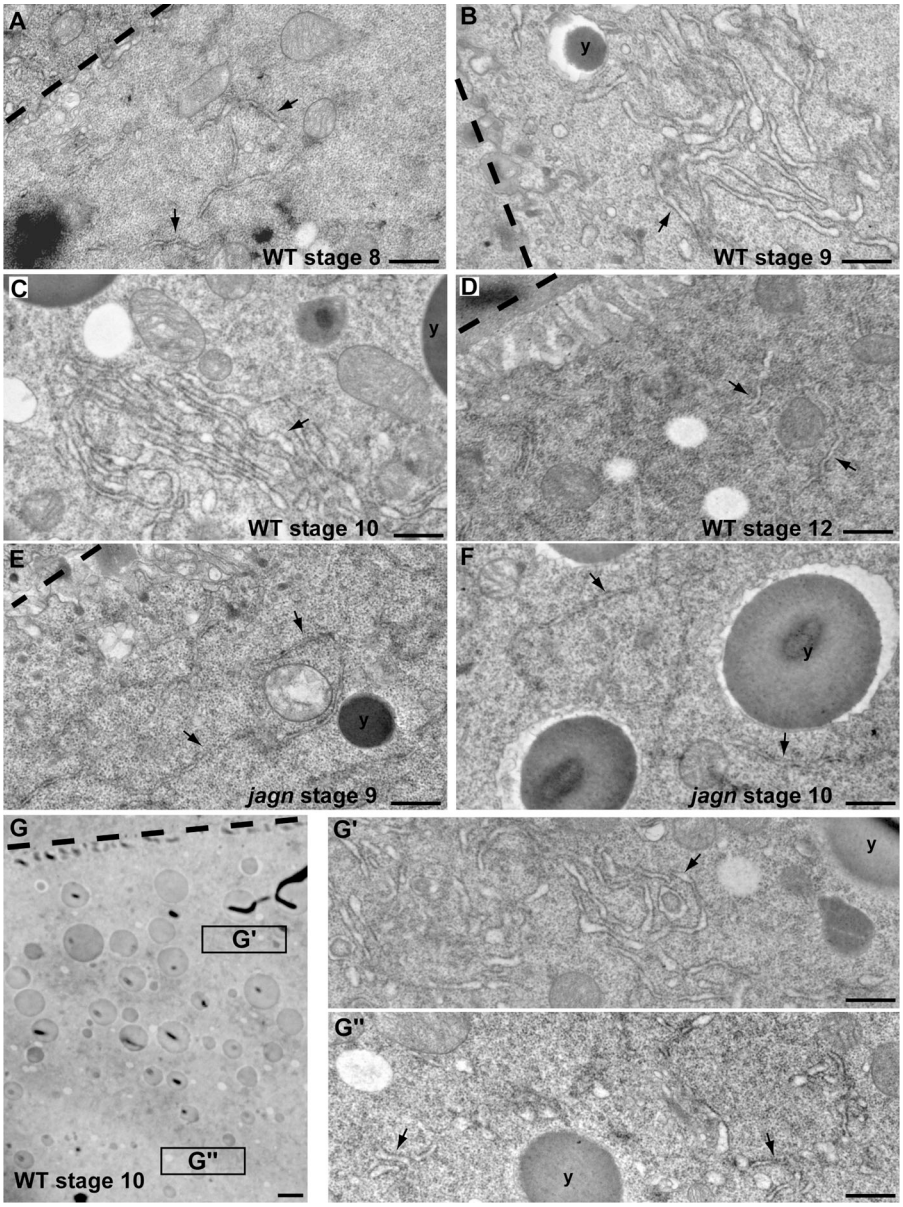

Figure 5. **Jagunal is required for ER clustering in the oocyte during vitellogenesis.** (A–D) EM images of progressive stages of wild-type egg chambers. During stage 8, the ER density is low and ER clusters are not found in the oocyte (A). ER clusters are formed in the oocyte, and the ER luminal space increases during stages 9 and 10 (B and C). ER clusters are not found in the oocyte during stage 12 (D). (E and F) EM images of stage 9 and 10 $jagn^{Q21X}$ GLCs. ER clusters are not found in *jagn* mutant oocytes, and the ER luminal space does not increase during stages 9 and 10 (E and F). (G) EM image of stage 10 oocyte. The ER density in the subcortical region (G′) is higher than inside of the ooplasm (G″). (A–G) Oocyte–follicle cell boundaries and yolk granules are marked by dashed lines and y's, respectively. Arrows indicate the ER. Bars: (A–F, G′, and G″) 0.5 μm; (G) 2 μm.

evenly distributed in the oocyte during stage 8, which is the earliest vitellogenic stage (Fig. 4 A). However, beginning at stage 9, EYFP-ER became concentrated in the oocyte subcortical region (Fig. 4 B, arrow), and the enrichment continued through stage 10 (Fig. 4 C, arrow), which is similar to distribution of Jagunal (Fig. 3, E and F). However, the enrichment of EYFP-ER in the subcortex was greatly reduced or eliminated in *jagn* GLCs (Fig. 4, E and F). We examined two other ER luminal proteins, protein disulfide isomerase (PDI)–GFP (Bobinnec et al., 2003) and Boca. Boca is an ER chaperone and is required for correct folding of Yolkless (Culi and Mann, 2003). Similar to EYFP-ER, these proteins also became concentrated in the oocyte subcortical region during stages 9 and 10 in wild-type egg chambers (Fig. 4, G and I, arrows). The enrichment of Boca and PDI-GFP was greatly reduced in *jagn* mutant oocytes; instead, the proteins were uniformly distributed in ooplasm (Fig. 4, H and J). We also examined two ER membrane proteins, Sec61-α-GFP and Rtnl1 (reticulon-like)-GFP. Sec61-α is a component of the translocon that translocates proteins across ER membranes (Johnson and van Waes, 1999), and reticulons are ubiquitous ER membrane proteins proposed to stabilize highly curved ER membrane tubules (Voeltz et al., 2006). Similar to ER luminal proteins, GFP fluorescence showed that these ER membrane proteins became concentrated in the oocyte subcortical region in wild-type egg chambers (Fig. 4, K and M, arrows), and the enrichment was again greatly reduced in *jagn* mutant oocytes (Fig. 4 liter and N). The concentration of all examined ER proteins in the oocyte subcortex suggests that the subcortical enrichment of ER proteins is not caused by uneven distribution of some ER proteins. Instead, the ER itself is likely to be concentrated in the subcortex. These results suggest that the ER is reorganized to produce a subcortical enrichment of the ER in the oocyte during vitellogenesis, and that Jagunal is required for this reorganization.

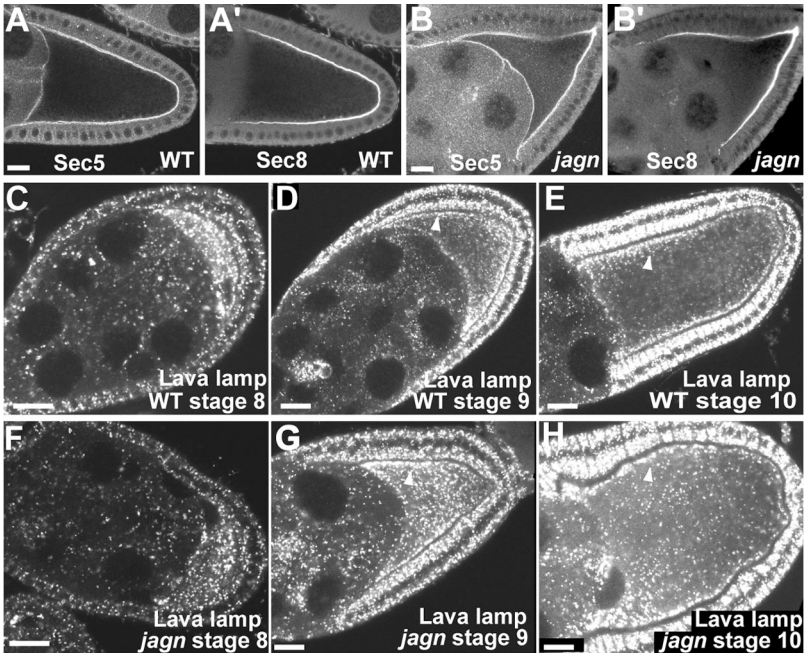

Figure 6. **Exocyst and Golgi complexes distribute normally in *jagn* mutant oocytes.** (A and B) Two exocyst components, Sec5 and Sec8, were examined in wild-type egg chambers (A) and $jagn^{Q21X}$ GLCs (B). In mutant oocytes, Sec5 and Sec8 localize normally at the cortex (B). Progressive stages of wild-type egg chambers (C–E) and $jagn^{Q21X}$ GLCs (F–H) were stained with Lava lamp antibodies to detect Golgi complexes. In wild-type stage 8 egg chambers, Golgi complexes are enriched in the oocyte and distributed evenly in the oocyte cytoplasm (C). During stages 9 and 10, many Golgi complexes accumulate near the oocyte cortex (D and E, arrowheads). In mutant oocytes, Golgi complex distribution is normal, with many Golgi complexes enriched in the subcortex (G and H, arrowhead). Bars, 20 μm.

Jagunal is required for clustering the ER in the oocyte during vitellogenesis

During stages 9 and 10, ER proteins were concentrated into clusters in the subcortex (Fig. 4 C′, arrow) in wild-type egg chambers. However, ER clusters were not found in *jagn* mutant oocyte subcortex (Fig. 4 F′). To further characterize ER organization in the oocyte during vitellogenesis, we examined ER organization in the ultrastructural level. In wild-type oocytes, the ER membranes were dispersed in the cytoplasm during stage 8 (Fig. 5 A, arrows). However, beginning at stage 9, many ER clusters were found in the subcortical region (Fig. 5 B, arrow), corresponding to ER clusters observed by confocal microscopy (Fig. 4 C′, arrow). Although some ER clusters were found far away from the oocyte cortex, the overall ER density was much lower deep inside the ooplasm (Fig. 5 G″) compared with the subcortical region (Fig. 5 G′), which is, again, consistent with the subcortical enrichment seen by confocal microscopy. The ER clusters continued to exist through stage 10 (Fig. 5 C, arrow). However, ER clusters were not found in stage 12 oocytes (Fig. 5 D, arrows), suggesting that the clusters disassembled after completion of vitellogenesis. In addition to ER clustering, ER morphology changed during vitellogenesis. The ER luminal space increased during stages 9 and 10 (Fig. 5, B and C), compared with stages 8 and 12 (Fig. 5, A and D). The swollen ER morphology might indicate high ER activity during stages 9 and 10.

The formation of ER clusters was severely impaired in *jagn* mutant oocytes. ER clusters were found in only 17% (3/18) of stage 9 and 10 *jagn* mutant oocytes; instead, the ER remained dispersed in the cytoplasm in most mutant oocytes (Fig. 5, E and F, arrows). Furthermore, the diameter of the ER lumen did not expand in *jagn* mutant oocytes compared with stage 9 and 10 wild-type oocytes (Fig. 5, E and F). These data show that Jagunal is required for the formation of ER clusters and ER morphology in the oocyte during vitellogenesis.

The distributions of exocyst and Golgi complexes are not affected in *jagn* mutant oocytes

The dramatic reorganization of the oocyte ER during stages 9 and 10 likely reflects a major increase in oocyte ER function needed for vitellogenesis and membrane expansion. To determine whether *jagn* mutations affect the organization of components downstream of ER in the exocytic membrane traffic pathway, we examined exocyst and Golgi complex localization. The exocyst complex is involved in targeting secretory vesicles to the appropriate exocytic sites on the plasma membrane (Guo et al., 2000), and two components of the exocyst complex, Sec5 and Sec8, localize at the oocyte plasma membrane (Fig. 6, A and A′; Murthy and Schwarz, 2004; Beronja et al., 2005). In contrast to Sec5, Sec8 does not localize at the interface of the oocyte and nurse cells (Beronja et al., 2005). Both Sec5 and Sec8 localized normally at the oocyte plasma membrane in *jagn* GLCs (Fig. 6, B and B′).

We used antibodies to Lava lamp, which is a golgin protein, to examine the distribution of Golgi complexes (Sisson et al., 2000; Papoulas et al., 2005). In wild-type egg chambers, Golgi complexes were enriched in the oocyte and distributed evenly throughout the ooplasm during stage 8 (Fig. 6 C), as previously reported (Herpers and Rabouille, 2004). However, we found that many Golgi complexes began to accumulate in the subcortical region during stage 9 (Fig. 6 D, arrowhead). The enrichment of Golgi complexes in the subcortical region became more evident during stage 10, with more Golgi near lateral plasma membranes compared with the posterior region (Fig. 6 E, arrowhead). Because enrichment of Golgi in the subcortical region was not previously reported (Herpers and Rabouille, 2004), we examined other Golgi markers, EYFP-Golgi (LaJeunesse et al., 2004) and dCOG5-GFP, which is a subunit of the COG complex (Farkas et al., 2003). These two proteins were also

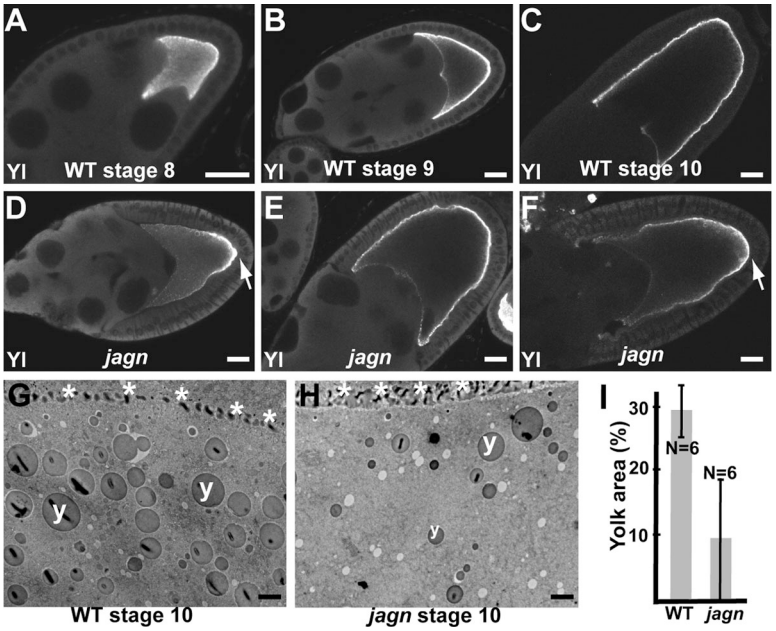

Figure 7. **Transport of Yolkless to the oocyte lateral membrane is reduced in *jagn* GLCs.** (A–F) Wild-type egg chambers (A–C) and $jagn^{Q21X}$ GLCs (D–F) were stained with Yolkless antibodies. Yolkless begins to be transported to the oocyte surface during stage 8 (A). During stages 9 and 10, Yolkless is localized at the oocyte cortex adjacent to follicle cells (B and C). In mutant oocytes (D–F), the intensity of Yolkless staining at the oocyte cortex is reduced. In most egg chambers the distribution of Yolkless is uneven, with the highest level at the posterior region (D and F, arrows). Yolkless enrichment at the posterior region is most evident during stage 9 (D). (G and H) EM images of a wild-type egg chamber (G) and a $jagn^{Q21X}$ GLC (H). Asterisks and y's mark oocyte–follicle cell boundary and yolk granules, respectively. (I) Quantitation of the percentage of yolk area in wild-type egg chambers and $jagn^{Q21X}$ GLCs. Percentage of yolk area was defined as the percentage of area occupied by yolk granules in the ooplasm. N indicates the number of examined oocytes. Bars: (A–F) 20 μm; (G and H) 2 μm.

enriched in the oocyte subcortex during stages 9 and 10 (unpublished data). However, unlike ER enrichment, the distribution of Golgi was unaffected in *jagn* mutant oocytes (Fig. 6, F–H).

The presence of exocyst complexes at the oocyte plasma membrane and Golgi enrichment in the oocyte subcortex during stages 9 and 10 support the idea that membrane traffic to the oocyte surface increases during these stages. However, our results indicate that exocyst and Golgi complex distribution is independent of the ER reorganization and clustering that requires Jagunal.

Transport of Yolkless to the oocyte surface is reduced in *jagn* mutant oocytes

Although Jagunal is conserved in metazoans, yeast do not have a Jagunal homologue, indicating that Jagunal is not an essential component of secretory pathway. Indeed, GLCs of *jagn* did not show any evident defect in previtellogenic stages, as do GLCs of *sec5* and *sec6* (Murthy and Schwarz, 2004; Beronja et al., 2005), suggesting that membrane trafficking is not blocked in mutant cells. Instead, Jagunal might be involved in increasing vesicular traffic to the oocyte surface during vitellogenesis by reorganizing the ER. To determine whether membrane traffic to the oocyte surface is reduced in *jagn* mutant oocytes during vitellogenesis, we examined the localization of Yolkless in *jagn* mutant oocytes. Yolkless is the yolk receptor, and its presence at the cell cortex coincides with vitellogenesis. Yolkless is distributed uniformly in the oocyte during previtellogenic stages and begins to be transported to the oocyte surface with the onset of vitellogenesis during stage 8 (Fig. 7 A; Schonbaum et al., 2000). Yolkless is transported to the oocyte plasma membrane by exocytosis, and it accumulates in the cortex as a result of endocytic recycling (Schonbaum et al., 2000). As oogenesis proceeds, the intensity of Yolkless at the cortex increases (Fig. 7 B); by stage 10, Yolkless is almost exclusively in the cortex (Fig. 7 C).

In *jagn* GLCs, the level of Yolkless in the oocyte lateral cortex was reduced (Fig. 7, D–F). The amount of Yolkless staining at the oocyte lateral cortex varied from near normal (Fig. 7 E) to absent (Fig. 7, D and F). Posterior enrichment of Yolkless in *jagn* mutant oocytes was most evident during stage 9 (Fig. 7 D, arrow), when 72% (39/54) of mutant oocytes showed a nonuniform cortical Yolkless distribution. Although we occasionally saw wild-type oocytes with a very weak posterior enrichment of Yolkless, the posterior enrichment of Yolkless was much stronger in *jagn* mutant oocytes. The behavior of Yolkless suggests that *jagn* mutations affect exocytic vesicular traffic to the oocyte lateral membrane. In addition, posterior enrichment of Yolkless in *jagn* mutant oocytes suggests the existence of a Jagunal-independent transport pathway polarized to the posterior pole. For example, the posterior enrichment of Yolkless may be caused, in part, by posterior-polarized endocytic recycling requiring Rab11 (Dollar et al., 2002).

To determine whether endocytosis of yolk is affected in *jagn* mutant oocytes, we examined yolk granules in electron micrographs of stage 10 wild-type and *jagn* mutant oocytes. Yolk granules were reduced in size and abundance in *jagn* mutant oocytes (Fig. 7, G and H). We measured the area of yolk granules in several egg chambers, and found that the overall area occupied by them was reduced by ~70% in *jagn* mutant oocytes (from 29 to 9.3%; Fig. 7 I). The amount of yolk in *jagn* oocytes varied widely, from 0 to 20% of oocyte area, but did not overlap wild-type amounts of yolk. To further examine endocytosis in *jagn* mutant oocytes, we quantitated the number of coated pits and vesicles in the plasma membrane and cortex of stage 10 oocytes. Compared with wild-type egg chambers (Fig. 8, B and C), the number of coated pits and vesicles was reduced by ~60% in *jagn* mutant oocytes (from 6.3 to 2.4 vesicles/μm; Fig. 8, D–F and G). Again, the amount of reduction varied, but numbers of coated pits and vesicles in *jagn* oocytes did not overlap wild type. These data show that yolk endocytosis and overall endocytic activity at the oocyte surface are reduced to similar extents in *jagn* mutant oocytes.

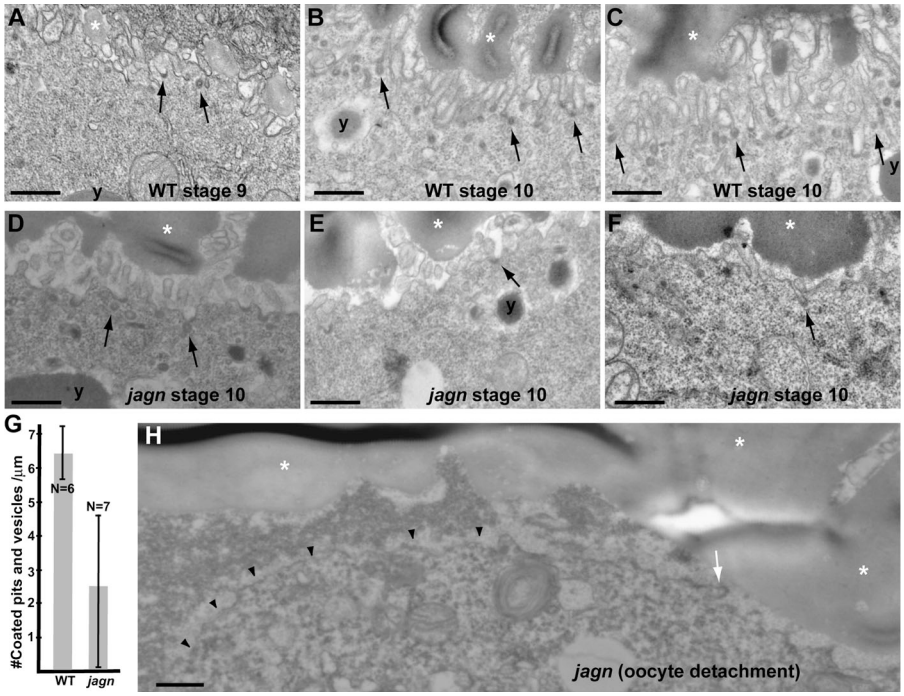

Figure 8. **Endocytosis and cell surface area is reduced in *jagn* mutant oocytes.** EM images of progressive stages of wild-type egg chambers (A–C) and stage 10 *jagn*^{Q21X} GLCs (D–F). Arrows indicate coated pits and vesicles. y's and asterisks mark yolk granules and vitelline bodies, respectively. In wild-type egg chambers, the oocyte surface has a high density of microvilli, and many coated pits and vesicles are found in the plasma membrane and cortex, especially during stage 10 (A–C). In *jagn* mutant oocytes, the density of microvilli is reduced to varying degrees, resulting in a decrease of the overall cell surface area (D–F). The number of coated pits and vesicles are also reduced in *jagn* mutant oocytes (D–F). (G) Quantitation of the number of coated pits and vesicles/micrometer. The number of coated pits and vesicles was counted and divided by the linear length of the examined oocyte surface. N indicates the number of examined oocytes. (H) An EM image of the anterior region of *jagn*^{Q21X} mutant oocyte. The plasma membrane of the mutant oocyte (arrowheads) is detached from neighboring cells. The number of microvilli (indicated by an arrow) is reduced. Bars, 0.5 µm.

Cell surface area is reduced in *jagn* mutant oocytes

Considering that Jagunal is an ER membrane protein and *jagn* mutations affect ER organization during vitellogenesis, the decreased endocytosis in *jagn* mutant oocytes is likely to be caused by reduced transport of factors required for endocytosis (including Yolkless and membrane) to the oocyte surface. Indeed, the surface area of *jagn* stage 10 oocytes (Fig. 8, D–F) was reduced compared with wild type (Fig. 8, B and C). Mutant oocytes ranged from a slight reduction in the number of microvilli (Fig. 8 D) to nearly absent microvilli (Fig. 8 F). Interestingly, we observed that microvilli were nearly absent on the surface of an oocyte that was detached from neighboring follicle cells (Fig. 8 H, arrowheads). The lack of sufficient membrane reserves in the form of microvilli could explain why the mutant oocytes fail to expand during stage 11.

Discussion

A large number of essential components of vesicular traffic have been identified through genetic and biochemical approaches, particularly in yeast, where defects in secretion cause striking phenotypes. However, proteins that play essential roles in regulating or organizing vesicular traffic, particularly in higher eukaryotes, still remain to be elucidated. Information is particularly limited in the context of development, where patterns of vesicle traffic are modified according to developmental programs. The *D. melanogaster* oocyte undergoes a dramatic transition in vesicular traffic during vitellogenesis, which, in addition to its large size, makes it an ideal model system to study how cells reorganize vesicular traffic. GLC analysis makes it possible to examine lethal mutations for effects on oocyte development, and allowed us to identify an essential gene, *jagunal*, which is required for ER organization. The amino acid sequence of Jagunal, as well as its localization, indicates that Jagunal is an ER membrane protein. The defects caused by *jagn* mutations can be explained by a failure to reorganize the ER at key developmental steps, resulting in reduced vesicular trafficking. In the oocyte, this reduced membrane traffic ultimately results in the dramatic failure in cell expansion that was observed initially. Our study suggests a functional role of ER reorganization in regulating exocytic vesicular traffic, and offers the opportunity to elucidate molecular mechanisms of organizing ER clusters.

Jagunal is required for clustering the ER

Many examples illustrating the importance of ER reorganization during cell differentiation exist; however, little is known about the molecular mechanisms used by cells to carry them out (Baumann and Walz, 2001). One well-documented example of ER reorganization occurs during oocyte maturation in diverse organisms (Kline, 2000). In mouse, 1–2-µm-wide ER clusters become localized in the oocyte cortex during oocyte maturation (Mehlmann et al., 1995). The cortical ER clusters are presumed to be involved in calcium signaling. Similar ER clusters that might be involved with calcium signaling were reported in *D. melanogaster* preblastoderm embryos (Frescas et al., 2006). ER clustering could be a general mechanism to establish a highly dense ER domain; therefore, determining the mechanisms cells use for this change in ER organization is of central interest. We found evidence that the ER becomes concentrated in the *D. melanogaster* oocyte subcortex during vitellogenesis, and accumulates into prominent clusters. The establishment of this highly dense ER domain requires Jagunal. Conservation of the *jagunal* gene in metazoans suggests a conserved role of Jagunal in ER clustering.

A possible function of Jagunal might be inferred from other proteins with four transmembrane domains. Diverse protein families have this organization, including tetraspanins, tetraspan vesicle membrane proteins, and junctional proteins of either the gap junction (connexins) or tight junction (claudins and occludins; Maecker et al., 1997; Tsukita and Furuse, 1999; Falk, 2000; Hubner et al., 2002). One of the most remarkable similarities of these diverse proteins is their tendency to occur as homomultimers in specialized membrane domains, where they are enriched in dense molecular aggregates (Hubner et al., 2002). It is therefore attractive to postulate that Jagunal exists as a homomultimeric complex and/or binds to other membrane proteins to form a protein complex on ER membrane. Jagunal contains several charged or polar amino acids in its transmembrane domains, many of which are conserved among Jagunal homologues; these amino acids might be involved in binding to other membrane proteins.

An intriguing feature of the amino acid sequence of Jagunal is the high conservation of the N-terminal 40 amino acids. The predicted topology of Jagunal places the amino terminus on the cytoplasmic side of the ER membrane. This domain could contribute to ER organization by binding cytoplasmic components such as cytoskeletal proteins, or by interacting with proteins within the ER that promote clustering. Identification of binding partners of the Jagunal N-terminal domain will provide clues to the role of Jagunal in ER reorganization.

Oocyte ER reorganization mirrors a change in the location of exocytosis during vitellogenesis

The phenotype of *jagn* germline clones reveals a modulation of ER function rather than a global block in membrane traffic. Mutations in exocyst components such as Sec5 and Sec6, which do block membrane traffic, cause a much more severe phenotype, in which egg chambers degenerate at an early stage (Murthy and Schwarz, 2004; Beronja et al., 2005). In contrast, previtellogenic egg chambers mutant for *jagn* are normal. More subtle effects on ER exit sites caused by *trailer hitch* mutations result in abnormal aggregates of Gurken and Yolkless in the cytoplasm of oocytes (Wilhelm et al., 2005), which we did not observe in *jagn* mutant oocytes. The transport of Yolkless to the oocyte lateral membrane is reduced in *jagn* mutant oocytes, but not blocked (Fig. 7), and Gurken transport is not affected (not depicted).

Our results suggest that membrane addition to the oocyte surface is reduced in *jagn* mutant oocytes. Decreased membrane addition might be caused by a defect in ER-derived exocytic membrane traffic or a defect in endocytic recycling. However, a defect in endocytic recycling in *jagn* mutant oocytes is unlikely because we did not see an accumulation of Yolkless in the cytoplasm, as was seen in *Rab11* and *sec5* mutants (Dollar et al., 2002; Sommer et al., 2005). Instead, Yolkless protein in *jagn* mutant oocytes remained cortical.

The oocyte plasma membrane is highly polarized in terms of membrane function during vitellogenesis. The anterior membrane is tightly attached to the four adjacent nurse cells and does not appear to be a site of active endocytosis. In contrast, the oocyte plasma membrane adjacent to follicle cells is highly endocytic with numerous pits or depressions of the plasma membrane between extensive microvilli (Giorgi and Jacob, 1977). The posterior of the oocyte is a special subdomain with elevated endocytic activity (Cummings and King, 1970; Dollar et al., 2002). In addition, there is evidence pointing to the existence of a special exocytic pathway in the oocyte posterior. When human transferrin receptor is expressed in the *D. melanogaster* oocyte, its trafficking to the cell surface is restricted to the posterior cortex of the oocyte during stage 8. The posterior enrichment of transferrin receptor at this stage is not dependent on its mRNA localization (Bretscher, 1996). Given that vitellogenesis begins during stage 8, this result suggests that vesicular traffic is initially polarized to the posterior pole until vitellogenesis starts. The posterior exocytic pathway might be used to transport Gurken at the posterior pole before stage 8 (Gonzalez-Reyes et al., 1995).

The role of Jagunal may be to facilitate the transition from posterior-polarized secretion during previtellogenic stages to a uniform level of membrane trafficking in the lateral and posterior endocytic oocyte membrane during vitellogenesis. More specifically, membrane traffic to the lateral endocytic membranes is particularly dependent on Jagunal function. Many *jagn* oocytes accumulate Yolkless at the posterior, but fail to provide sufficient Yolkless to lateral endocytic membrane. The formation of the lateral endocytic subdomain coincides with the establishment of a subcortical ER domain and the enrichment of Golgi complexes near the endocytic membrane. The coincidence suggests that the ER and Golgi complexes in the subcortical region are involved in massive vesicular traffic to the plasma membrane adjacent to follicle cells. Jagunal may be involved in establishing a subcortical ER domain by clustering the ER in the subcortical region to increase ER density and vesicular traffic. The disappearance of ER clusters before stage 12 of oogenesis further suggests a specific role of ER clusters during vitellogenesis.

Interestingly, the enrichment of Golgi complexes in the subcortical region does not require *jagn*, suggesting that subcortical Golgi enrichment is not dependent on the subcortical ER. Golgi complexes might move to the oocyte subcortex along microtubules, as they do in *D. melanogaster* embryos (Papoulas et al., 2005).

Jagunal is required for oocyte and bristle growth

This study revealed that Jagunal is involved with ER reorganization; however, the final outcome for mutant oocytes and bristle cells is a failure to grow during development. Therefore, we need to understand how a defect in ER reorganization ultimately results in a growth defect. Previously characterized mutations that affect oocyte growth impede the flow of cytoplasm from nurse cells into the oocyte by affecting functions of nurse cells (Hudson and Cooley, 2002), emphasizing that nurse cell cytoplasm is essential for oocyte growth. However, the surface of the oocyte itself also has to expand to accommodate oocyte growth. This is especially critical during the final, rapid phase of nurse cell cytoplasm transport (dumping) that occurs during

the 30-min stage 11. The oocyte surface also must more than double in size during this short time.

There are at least two plausible mechanisms for providing enough membrane to the oocyte surface during dumping, either of which could require Jagunal. The first model is that membrane is added to the plasma membrane rapidly, perhaps by massive vesicle fusion. Given that ooplasm streams vigorously in the oocyte during this time (Serbus et al., 2005), membrane reservoirs must exist near the cortex, where streaming does not occur. The second model is that a surplus of membrane is stored in advance as microvilli. In this model, the oocyte can expand rapidly by using the membrane of some microvilli during stage 11. If the ability to add membrane before or during dumping is reduced in *jagn* mutant oocytes, the rapid influx of nurse cell cytoplasm might result in excessive tension on the plasma membrane, finally causing detachment from adjacent cells and growth arrest.

Similar models for membrane addition have been considered for *D. melanogaster* cellularization, when the membrane surface area increases 25-fold in about 1 h (Fullilove and Jacobson, 1971; Turner and Mahowald, 1976; Loncar and Singer, 1995). Several lines of evidence support a dominant role of membrane trafficking for this process. For example, pulse-labeling experiments in living embryos showed polarized insertion of new membrane from a cytoplasmic reservoir during cellularization (Lecuit and Wieschaus, 2000). In addition, injection of brefeldin A, which inhibits ER–Golgi transport, reduces the speed of membrane invagination (Sisson et al., 2000). An open question is whether the organization of ER is important for membrane traffic during cellularization. Interestingly, before cellularization occurs, the ER becomes segregated into discrete units associated with each nucleus, ensuring that cells receive equal amounts of ER (Bobinnec et al., 2003; Frescas et al., 2006). It will be interesting to determine whether this organization is crucial to membrane addition during cellularization, and if Jagunal is involved in creating the ER units.

Bristle growth is also affected by *jagn* mutations, suggesting that Jagunal participates more generally in rapid cell growth. Both the small bristle phenotype and the defect in bristle ridge structure can be explained by reduced membrane trafficking. During pupal development, tiny bristles sprout and elongate for ~16 h to reach their maximum length (65 μm for microchaetes or 400 μm for macrochaetes; Tilney et al., 1996). Thus, bristles elongate at an average rate of 4 μm/h (microchaetes) or 25 μm/h (macrochaetes) during the elongation period. Accordingly, a large amount of membrane must be added to the plasma membrane to accommodate this growth, and our results suggest a requirement for Jagunal during this process. Future work will be important to determine whether ER reorganization and elevated membrane traffic underlie bristle growth.

Materials and methods

Genetics/fly strains

All crosses and culturing of *D. melanogaster* were performed using standard procedures (Ashburner, 1989). Canton-S and w^{1118} flies were used as wild-type controls. The first *jagunal* allele ($jagn^{Q21X}$) described in this study was from a subset of lethal mutations on chromosome 3R (Yohn et al., 2003) selected by R. Lehmann (New York University, New York, NY) because germline clones produced small eggs. We made four more alleles of *jagn* with an ethylmethane sulphonate noncomplementation-lethal screen. EYFP-ER and -Golgi flies (LaJeunesse et al., 2004) were obtained from the Bloomington Stock Center (Indiana University, Bloomington, IN). The dCOG5-GFP (GFP-Fws) fly stock was obtained from M. Fuller (Stanford University, Palo Alto, CA; Farkas et al., 2003). Bsg-GFP (G00413), PDI-GFP (ZCL1503), Rtnl1-GFP (ZCL1569), and Sec61α-GFP (ZCL0488) flies were generated by protein trap screening (Morin et al., 2001). The *actin-Gal4* driver (Ito et al., 1997) or germline triple driver (a combination of *pCOG-Gal4:VP16* [Rorth, 1998], *NGT40* [Tracey et al., 2000], and *nos-Gal4-VP16* [Van Doren et al., 1998]) were used to induce ubiquitous or germline-specific expression, respectively, of pUASp-Jagunal in the ovary. Flies used for clonal analysis were obtained from the Bloomington Stock Center.

Construction of transgenes and generation of transgenic lines

A cDNA clone of *jagunal* (1.1 kb) was obtained by RT-PCR and subcloned into pUASp, creating *P{UASp-Jagunal}*. To make the Jagn-GFP and -Venus constructs, a genomic DNA (6 kb) was used. GFP was inserted at the C terminus, and Venus was inserted between the first and second transmembrane domains. The Jagn-GFP and -Venus constructs were subcloned into CaSpeR, creating *P{CaSpeR-Jagn-GFP}* and *P{CaSpeR-Jagn-Venus}*.

Clonal analysis

All *jagn* alleles were induced on a $P\{FRT\}^{3R\text{-}82B}$ chromosome (Xu and Rubin, 1993). For clones marked by loss of ovo^{D} (Chou et al., 1993), second–third instar larvae of the genotype $P\{hsFLP\}/+;\ jagn,\ P\{FRT\}^{3R\text{-}82B}/P\{ovo^{D1\text{-}18}\}3R,\ P\{FRT\}^{3R\text{-}82B}$ were heat shocked for 1–2 h in a 38°C water bath on two consecutive days. Ovaries were dissected from female flies that were fed yeast paste for ~7 d to dilute out wild-type gene products. To mark bristle clones, flies carrying mutations were crossed to $y\ P\{hsFLP\};\ P\{y^{+}\},P\{FRT\}^{3R\text{-}82B}$ flies, and their progeny were heat shocked as first–second instar larvae for 1–2 h in a 38°C water bath. To overexpress Jagunal in a mosaic manner, *UAS-GFPnls, UASp-Jagn* flies were crossed to $P\{hsFLP\};\ P\{actin{>}y^{+}{>}Gal4\}$ flies (Ito et al., 1997), and their progeny were heat shocked as second–third instar larvae for 1–2 h in a 38°C water bath.

Antibody production for Jagunal

Anti-Jagunal antibody was raised against the C-terminal 17 amino acids. Purified peptide antigen, CYNLVKAWKARTATRKFQ, was obtained from the Keck Biotechnology Resource Laboratory (Yale University, New Haven, CT). The antigen was injected into a rabbit and boosted four times according to a standard protocol (Cocalico Biologicals, Inc.). Antibodies were purified with a Sulfolink kit (Pierce Chemical Co.) using the original peptide.

Immunocytochemistry and confocal microscopy

Ovaries were dissected in IMADS (Singleton and Woodruff, 1994) and fixed in 6% formaldehyde saturated with heptane as previously described (Verheyen and Cooley, 1994). To visualize F-actin, egg chambers were incubated with 1 U of rhodamine-conjugated phalloidin in PBT. The following antibodies were used: rabbit anti-Jagunal at 1:200 (this study), mouse monoclonal anti–Hts-RC at 1:10 (Robinson et al., 1994), rabbit anti–Lava lamp at 1:200 (from John Sisson, University of Texas, Austin, TX; Sisson et al., 2000), rat anti-Yolkless at 1:200 (from Christopher Schonbaum, University of Chicago, Chicago, IL; Schonbaum et al., 2000), mouse monoclonal anti-Sec5 at 1:200 (from Thomas Schwarz, Harvard University, Boston, MA; Murthy and Schwarz, 2004), guinea pig anti-Sec8 at 1:1,000 (from Ulrich Tepass, University of Toronto, Toronto, Ontario, Canada; Beronja et al., 2005), guinea pig anti-Boca at 1:500 (from Richard Mann, Columbia University, New York, NY; Culi and Mann, 2003), and rabbit anti-GFP at 1:500 (Torrey Pines Biolabs, Inc.). Anti-GFP antibodies were used to stain EYFP-ER, Jagn-GFP, and Jagn-Venus. Fluorescence micrographs were obtained at room temperature using an inverted microscope (Axiovert 100M; Carl Zeiss MicroImaging, Inc.) equipped with a laser scanning confocal imaging system (LSM510; Carl Zeiss MicroImaging, Inc.) and a 40×/1.2 NA water-immersion objective lens (C-Apochromat; Carl Zeiss MicroImaging, Inc.; Center for Cell and Molecular Imaging, Yale University School of Medicine, New Haven, CT). Images were processed using Photoshop (Adobe) and assembled in Illustrator (Adobe).

Western blot analysis

Dissected ovaries were homogenized in SDS loading buffer and boiled for 5 min. Equal amounts of ovary extract were loaded and separated on a

12% polyacrylamide gel. Proteins were transferred to nitrocellulose, blocked with 5% milk, and probed with primary antibodies overnight at 4°C. Rabbit anti-Jagunal antibody was used at 1:2,000.

Scanning EM

Flies were put through an EtOH dehydration series (25, 50, 75, and 100%), followed by treatment with hexamethyldisilazane. The treated flies were dried in a low vacuum overnight. Flies were mounted on stubs, rotary shadowed, and viewed on an ISI SS-40 scanning electron microscope (Department of Molecular, Cellular and Developmental Biology EM Facility, Yale University). Images were recorded onto Polaroid 53 film and scanned at 300 dpi.

Transmission EM

Ovaries were dissected in IMADS (Singleton and Woodruff, 1994), fixed in 2% glutaraldehyde in 0.1 M sodium cacodylate buffer, pH 7.4, for 1 h. After washing with 0.1 M sodium cacodylate buffer overnight, samples were postfixed in 1% osmium tetroxide in 0.1 M sodium cacodylate buffer for 1 h. After making sections, they were stained with 2% uranyl acetate for 5 min and 1% lead citrate for 2.5 min and examined in a Tecnai 12 Biotwin electron microscope (Center for Cell and Molecular Imaging, Yale University School of Medicine, New Haven, CT). Digital images were collected with a Morada charge-coupled device camera using iTEM software (Olympus). To quantitate the percentage of yolk area in electron micrographs of oocytes, regions of ooplasm were selected and the areas of yolk granules within the selected regions was measured using ImageJ v. 1.36b (National Institutes of Health). Coated pits and vesicles were counted in selected cortical region of oocytes. The linear length of the selected oocyte surface (excluding microvillar surface) was measured using ImageJ.

Online supplemental material

Ovaries expressing Bsg-GFP were dissected in mineral oil and ovarioles were spread well on the coverslip. Immediately after dissection, GFP fluorescence was visualized on a LSM 510 confocal microscope with a 20× objective. Images were collected every 20 s for 30–60 min. The images were converted to a movie using Graphic Converter (Lemkesoft). Movies are 240 times faster than real time. Wild-type egg chambers (Video 1) and *jagn*^{Q21X} GLCs (Videos 2 and 3) are presented. The online version of this article is available at http://www.jcb.org/cgi/content/full/jcb.200701048.

We thank Ruth Lehmann for giving us her collection of small egg mutants on chromosome 3R. We thank Christopher Schonbaum, John Sisson, Richard Mann, Thomas Schwarz, and Ulrich Tepass for sending antibodies, and Minx Fuller and the Bloomington Stock Center for fly stocks. We thank Marc Pypaert (Yale Center for Cell and Molecular Imaging) for help with EM. We thank members of the Cooley laboratory for advice and comments on the manuscript.

This work was supported by a National Institutes of Health grant (GM043301) to L. Cooley.

Submitted: 9 January 2007
Accepted: 12 February 2007

References

Ashburner, M. 1989. *Drosophila*: A Laboratory Handbook. Cold Spring Harbor Laboratory Press, Cold Spring Harbor, New York.

Baumann, O., and B. Walz. 2001. Endoplasmic reticulum of animal cells and its organization into structural and functional domains. *Int. Rev. Cytol.* 205:149–214.

Beronja, S., P. Laprise, O. Papoulas, M. Pellikka, J. Sisson, and U. Tepass. 2005. Essential function of *Drosophila* Sec6 in apical exocytosis of epithelial photoreceptor cells. *J. Cell Biol.* 169:635–646.

Bobinnec, Y., C. Marcaillou, X. Morin, and A. Debec. 2003. Dynamics of the endoplasmic reticulum during early development of *Drosophila melanogaster*. *Cell Motil. Cytoskeleton*. 54:217–225.

Bretscher, M.S. 1996. Expression and changing distribution of the human transferrin receptor in developing *Drosophila* oocytes and embryos. *J. Cell Sci.* 109:3113–3119.

Chou, T.B., E. Noll, and N. Perrimon. 1993. Autosomal *P[ovoD1]* dominant female-sterile insertions in *Drosophila* and their use in generating germline chimeras. *Development*. 119:1359–1369.

Culi, J., and R.S. Mann. 2003. Boca, an endoplasmic reticulum protein required for wingless signaling and trafficking of LDL receptor family members in *Drosophila*. *Cell*. 112:343–354.

Cummings, M.R., and R.C. King. 1970. The cytology of the vitellogenic stages of oogenesis in *Drosophila melanogaster*. II. Ultrastructural investigations on the orgin of protein yolk spheres. *J. Morphol.* 130:467–478.

Dollar, G., E. Struckhoff, J. Michaud, and R.S. Cohen. 2002. Rab11 polarization of the *Drosophila* oocyte: a novel link between membrane trafficking, microtubule organization, and *oskar* mRNA localization and translation. *Development*. 129:517–526.

Falk, M.M. 2000. Biosynthesis and structural composition of gap junction intercellular membrane channels. *Eur. J. Cell Biol.* 79:564–574.

Farkas, R.M., M.G. Giansanti, M. Gatti, and M.T. Fuller. 2003. The *Drosophila* Cog5 homologue is required for cytokinesis, cell elongation, and assembly of specialized Golgi architecture during spermatogenesis. *Mol. Biol. Cell*. 14:190–200.

Flucher, B.E. 1992. Structural analysis of muscle development: transverse tubules, sarcoplasmic reticulum, and the triad. *Dev. Biol.* 154:245–260.

Frescas, D., M. Mavrakis, H. Lorenz, R. Delotto, and J. Lippincott-Schwartz. 2006. The secretory membrane system in the *Drosophila* syncytial blastoderm embryo exists as functionally compartmentalized units around individual nuclei. *J. Cell Biol.* 173:219–230.

Fullilove, S.L., and A.G. Jacobson. 1971. Nuclear elongation and cytokinesis in *Drosophila montana*. *Dev. Biol.* 26:560–577.

Giorgi, F., and J. Jacob. 1977. Recent findings on oogenesis of *Drosophila melanogaster*. I. Ultrastructural observations on the developing ooplasm. *J. Embryol. Exp. Morphol.* 38:115–124.

Gonzalez-Reyes, A., H. Elliott, and D. St Johnston. 1995. Polarization of both major body axes in *Drosophila* by gurken-torpedo signalling. *Nature*. 375:654–658.

Guo, W., M. Sacher, J. Barrowman, S. Ferro-Novick, and P. Novick. 2000. Protein complexes in transport vesicle targeting. *Trends Cell Biol.* 10:251–255.

Herpers, B., and C. Rabouille. 2004. mRNA localization and ER-based protein sorting mechanisms dictate the use of transitional endoplasmic reticulum-golgi units involved in gurken transport in *Drosophila* oocytes. *Mol. Biol. Cell*. 15:5306–5317.

Hubner, K., R. Windoffer, H. Hutter, and R.E. Leube. 2002. Tetraspan vesicle membrane proteins: synthesis, subcellular localization, and functional properties. *Int. Rev. Cytol.* 214:103–159.

Hudson, A.M., and L. Cooley. 2002. Understanding the function of actin-binding proteins through genetic analysis of *Drosophila* oogenesis. *Annu. Rev. Genet.* 36:455–488.

Ito, K., W. Awano, K. Suzuki, Y. Hiromi, and D. Yamamoto. 1997. The *Drosophila* mushroom body is a quadruple structure of clonal units each of which contains a virtually identical set of neurones and glial cells. *Development*. 124:761–771.

Jackson, M.R., T. Nilsson, and P.A. Peterson. 1993. Retrieval of transmembrane proteins to the endoplasmic reticulum. *J. Cell Biol.* 121:317–333.

Johnson, A.E., and M.A. van Waes. 1999. The translocon: a dynamic gateway at the ER membrane. *Annu. Rev. Cell Dev. Biol.* 15:799–842.

Kline, D. 2000. Attributes and dynamics of the endoplasmic reticulum in mammalian eggs. *Curr. Top. Dev. Biol.* 50:125–154.

LaJeunesse, D.R., S.M. Buckner, J. Lake, C. Na, A. Pirt, and K. Fromson. 2004. Three new *Drosophila* markers of intracellular membranes. *Biotechniques*. 36:784–790.

Lecuit, T., and E. Wieschaus. 2000. Polarized insertion of new membrane from a cytoplasmic reservoir during cleavage of the *Drosophila* embryo. *J. Cell Biol.* 150:849–860.

Loncar, D., and S.J. Singer. 1995. Cell membrane formation during the cellularization of the syncytial blastoderm of *Drosophila*. *Proc. Natl. Acad. Sci. USA*. 92:2199–2203.

Maecker, H.T., S.C. Todd, and S. Levy. 1997. The tetraspanin superfamily: molecular facilitators. *FASEB J.* 11:428–442.

Mahajan-Miklos, S., and L. Cooley. 1994. Intercellular cytoplasm transport during *Drosophila* oogenesis. *Dev. Biol.* 165:336–351.

Mahowald, A.P. 1972. Ultrastructural observations on oogenesis in *Drosophila*. *J. Morphol.* 137:29–48.

Mehlmann, L.M., M. Terasaki, L.A. Jaffe, and D. Kline. 1995. Reorganization of the endoplasmic reticulum during meiotic maturation of the mouse oocyte. *Dev. Biol.* 170:607–615.

Morin, X., R. Daneman, M. Zavortink, and W. Chia. 2001. A protein trap strategy to detect GFP-tagged proteins expressed from their endogenous loci in *Drosophila*. *Proc. Natl. Acad. Sci. USA*. 98:15050–15055.

Murthy, M., and T.L. Schwarz. 2004. The exocyst component Sec5 is required for membrane traffic and polarity in the *Drosophila* ovary. *Development*. 131:377–388.

Nilsson, T., M. Jackson, and P.A. Peterson. 1989. Short cytoplasmic sequences serve as retention signals for transmembrane proteins in the endoplasmic reticulum. *Cell*. 58:707–718.

Overton, J. 1967. The fine structure of developing bristles in wild type and mutant *Drosophila melanogaster*. *J. Morphol.* 122:367–379.

Papoulas, O., T.S. Hays, and J.C. Sisson. 2005. The golgin Lava lamp mediates dynein-based Golgi movements during *Drosophila* cellularization. *Nat. Cell Biol.* 7:612–618.

Robinson, D.N., and L. Cooley. 1996. Stable intercellular bridges in development: the cytoskeleton lining the tunnel. *Trends Cell Biol.* 6:474–479.

Robinson, D.N., K. Cant, and L. Cooley. 1994. Morphogenesis of *Drosophila* ovarian ring canals. *Development*. 120:2015–2025.

Rorth, P. 1998. Gal4 in the *Drosophila* female germline. *Mech. Dev.* 78:113–118.

Schonbaum, C.P., J.J. Perrino, and A.P. Mahowald. 2000. Regulation of the vitellogenin receptor during *Drosophila melanogaster* oogenesis. *Mol. Biol. Cell*. 11:511–521.

Serbus, L.R., B.J. Cha, W.E. Theurkauf, and W.M. Saxton. 2005. Dynein and the actin cytoskeleton control kinesin-driven cytoplasmic streaming in *Drosophila* oocytes. *Development*. 132:3743–3752.

Singleton, K., and R.I. Woodruff. 1994. The osmolarity of adult *Drosophila* hemolymph and its effect on oocyte-nurse cell electrical polarity. *Dev. Biol.* 161:154–167.

Sisson, J.C., C. Field, R. Ventura, A. Royou, and W. Sullivan. 2000. Lava lamp, a novel peripheral Golgi protein, is required for *Drosophila melanogaster* cellularization. *J. Cell Biol.* 151:905–918.

Sommer, B., A. Oprins, C. Rabouille, and S. Munro. 2005. The exocyst component Sec5 is present on endocytic vesicles in the oocyte of *Drosophila melanogaster. J. Cell Biol.* 169:953–963.

Teasdale, R.D., and M.R. Jackson. 1996. Signal-mediated sorting of membrane proteins between the endoplasmic reticulum and the Golgi apparatus. *Annu. Rev. Cell Dev. Biol.* 12:27–54.

Tilney, L.G., P. Connelly, S. Smith, and G.M. Guild. 1996. F-actin bundles in *Drosophila* bristles are assembled from modules composed of short filaments. *J. Cell Biol.* 135:1291–1308.

Tracey, W.D., Jr., X. Ning, M. Klingler, S.G. Kramer, and J.P. Gergen. 2000. Quantitative analysis of gene function in the *Drosophila* embryo. *Genetics*. 154:273–284.

Tsukita, S., and M. Furuse. 1999. Occludin and claudins in tight-junction strands: leading or supporting players? *Trends Cell Biol.* 9:268–273.

Turner, F.R., and A.P. Mahowald. 1976. Scanning electron microscopy of *Drosophila* embryogenesis. 1. The structure of the egg envelopes and the formation of the cellular blastoderm. *Dev. Biol.* 50:95–108.

Van Doren, M., A.L. Williamson, and R. Lehmann. 1998. Regulation of zygotic gene expression in *Drosophila* primordial germ cells. *Curr. Biol.* 8:243–246.

Verheyen, E., and L. Cooley. 1994. Looking at oogenesis. *Methods Cell Biol.* 44:545–561.

Voeltz, G.K., W.A. Prinz, Y. Shibata, J.M. Rist, and T.A. Rapoport. 2006. A class of membrane proteins shaping the tubular endoplasmic reticulum. *Cell*. 124:573–586.

Wilhelm, J.E., M. Buszczak, and S. Sayles. 2005. Efficient protein trafficking requires trailer hitch, a component of a ribonucleoprotein complex localized to the ER in *Drosophila*. *Dev. Cell*. 9:675–685.

Xu, T., and G.M. Rubin. 1993. Analysis of genetic mosaics in developing and adult *Drosophila* tissues. *Development*. 117:1223–1237.

Yohn, C.B., L. Pusateri, V. Barbosa, and R. Lehmann. 2003. l(3)malignant brain tumor and three novel genes are required for *Drosophila* germ-cell formation. *Genetics*. 165:1889–1900.